Electronic Supplementary Material (ESI) for Inorganic Chemistry Frontiers.

Highly efficient water splitting over RuO_2/F-doped graphene electrocatalyst with ultra-low ruthenium content

Zhenglong Fan, Fan Liao, Huixian Shi, Yang Liu*, Mingwang Shao* and Zhenhui Kang*

Institute of Functional Nano & Soft Materials (FUNSOM), Jiangsu Key Laboratory for Carbon-Based Functional Materials & Devices, Soochow University, Suzhou 215123, P. R. China.

Experimental

Materials

Ruthenium chloride ($RuCl_3$) was purchased from Aladdin Industrial Corporation. Nafion (5 wt%) was obtained from Sigma-Aldrich Co. Graphene oxide (GO) was supported by Advanced Materials Supplier Co. The commercial Pt/C catalyst was from Alfa Aesar Co. (Platinum, nominally 40 wt% on carbon black). Commeical RuO_2 was bought from Great Chemicals Co. Other reagents were analytical reagent grade without further purification. Doubly-distilled water was used throughout the experiment.

Characterization

X-ray powder diffraction (XRD, Philips X'pert PRO MPD diffractometer) with Cu Kα radiation source (λ_{Cu} = 0.15406 nm) was used to study the phase and crystallography of the catalysts. Transmission electron microscope (TEM) (FEI Tecnai G2 F20 S-TWIN) and high resolution TEM (HRTEM) were used to observe the morphology of the surface of catalyst with an accelerating voltage of 200 kV. Thermogravimetric analysis (TGA) was used to measure the content of RuO_2 in the catalyst under 900 °C with the heating rate of 10 °C per minute under air. The states of catalysts were analyzed by using X-ray photoelectron spectroscopy (XPS) on a Kratos AXIS UltraDLD ultrahigh vacuum surface analysis system with Al Kα radiation (1486 eV) as a probe. Scanning electron microscopy (SEM) was performed

via using a Zeiss Supra 55. The Fourier transform infrared spectrum (FTIR) (HYPERION Bruker) was used to Vibration of chemical bonds. The mass ratios of Ru in catalysts were characterized by Bruker Aurora M90 inductively coupled plasma mass spectrometer (ICP-MS).

Synthesis of SiNWs

SiNWs was obtained via thermal-evaporation oxide-assisted growth method [S1]. In brief, load 500 mg SiO powder on alumina boat, then put it at the center of a horizontal alumina tube mounted inside a high-temperature tube furnace. The reaction pressure was maintained at 0.8 Torr by using a mechanical pump. The temperature was heated at a rate of 5 °C and maintaining 1280 °C for 3 h. The product was obtained from the surface of the alumina tube.

Electrochemical activation of RuO_2/F-graphene for OER

According to previous reports, RuO_2/F-graphene catalysts need to be activated by electrochemical activated process before OER test. The RuO_2/F-graphene catalysts were activated in the potential cycling from +0.05 V to +1.5 V at rate of 50 mV s^{-1} for about 20 cycles until reproducible voltammograms were obtained [S2].

Electrochemical measurements

CHI 760 D electrochemical workstation with a standard three-electrode system was used to conduct all HER and OER electrochemical experiments. A modified glassy carbon electrode (GCE, 3 mm in diameter) and Ag/AgCl (3 M KCl solution) electrode are chosen to be the working electrode and the reference electrode, respectively. A carbon rob (for HER) or a Pt wire (for OER) were selected to be the counter electrode.

The preparation of working electrode was as follow: First, 2 mg catalyst was added into mixed solution (900 μL N,N-dimethylformamide and 100 μL Nafion solution (0.5 wt%)), then the dispersion was ultrasonicated until it become homogeneous. Finally, 4 μL of above dispersion was dropped on the surface of glassy carbon

electrode. The equation (E_{RHE} = E(vs. $Ag/AgCl_2$) + 0.197 V + 0.0591 V × pH) was used to calibrate data and convert to the reversible hydrogen electrode (RHE).

All electrochemical measurements were studied at room temperature. OER and HER performances were analyzed in 1 M KOH solution or 1 M PBS (pH = 7.3) solution, respectively. Linear sweep voltammetry (LSV) with scan rate of 5 mV s^{-1} was used to conduct all catalysts electrocatalytic performance. The experiment of overall water splitting was carried out in a two-electrode system. Both cathode and anode were served by catalysts modified GCEs. The stability of all catalysts was examined for HER and OER by chronopotentiometry. In brief, The current density of working electrode was maintained in 10 mA·cm^{-2} during whole test process and operating potentials were regarded as a function of time.

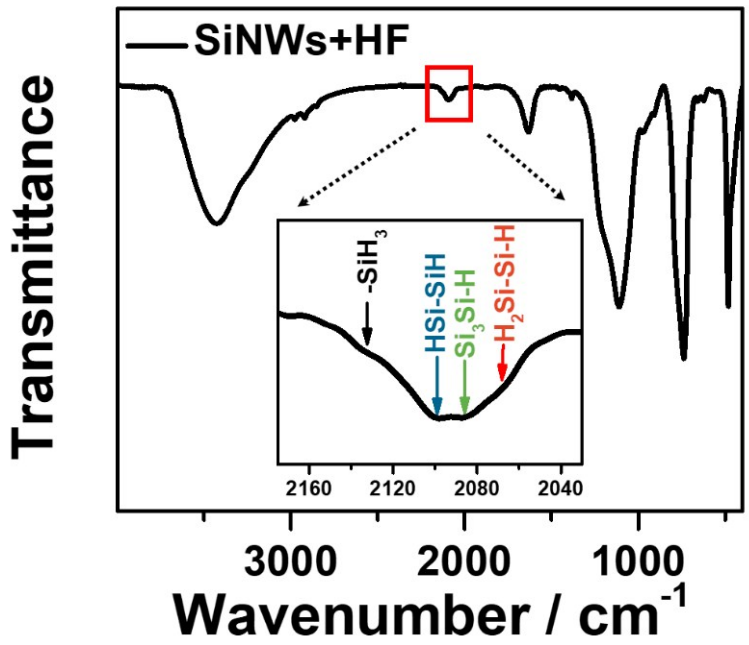

Figure S1. The FTIR of SiNWs with HF treatment; inset is the enlarged view with wavenumber from 2120 to 2180 cm^{-1}.

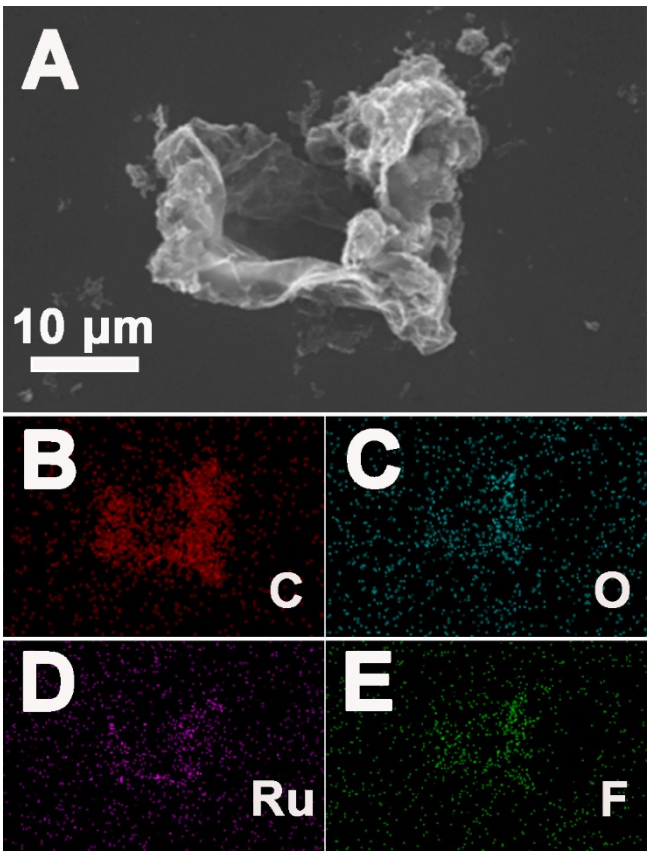

Figure S2. Characterization of SEM. (A) SEM image of RuO_2/F-graphene; and (B-E) corresponding EDS mapping for distribution of C, O, Ru and F elements.

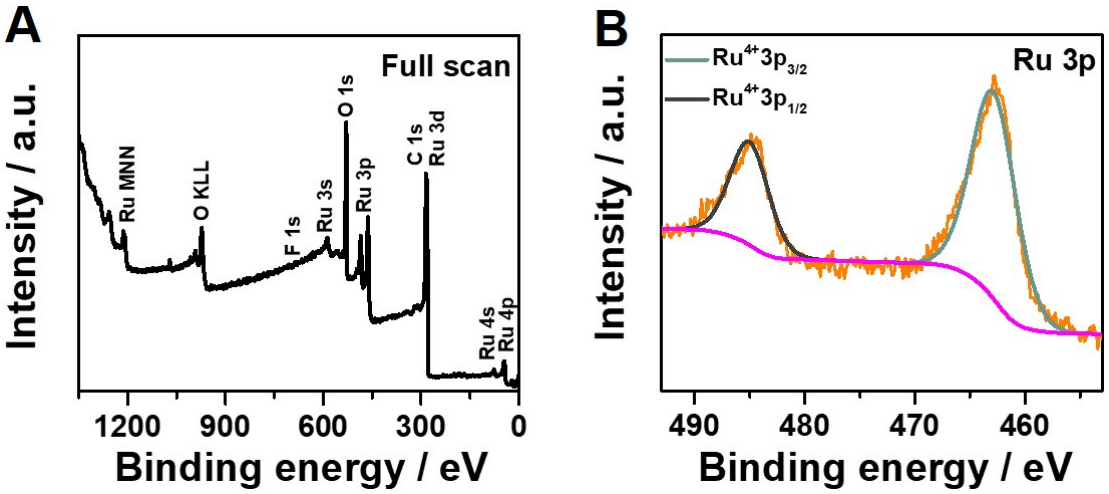

Figure S3. (A) the full scan XPS spectrum of RuO_2/F-graphene; (B) the high-resolution Ru 3p spectrum of RuO_2/F-graphene.

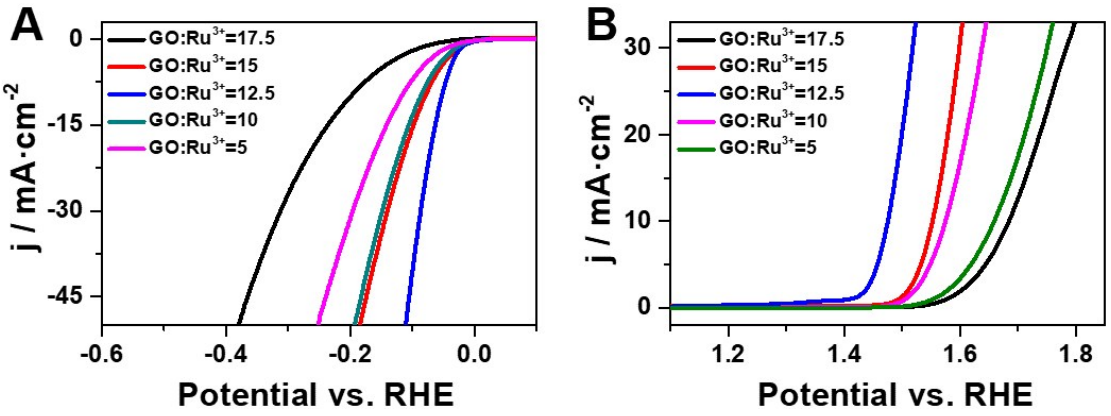

Figure S4. LSV curves of catalysts with different mass ratio (GO:Ru^{3+}) in 1 M KOH solution. (A) for HER and (B) for OER.

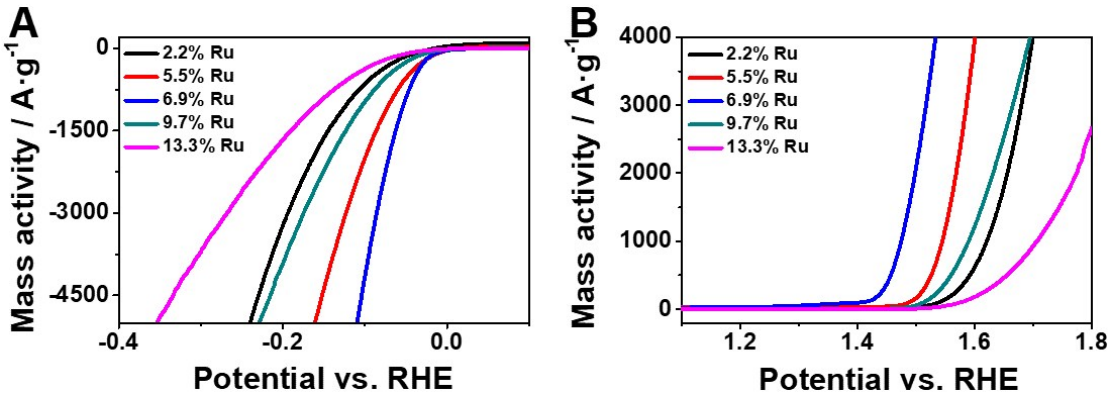

Figure S5. Mass activity based on the weight of Ru at different potentials of RuO_2/F-graphene catalysts in 1 M KOH solution. (A) for HER and (B) for OER. The mass ratios of Ru in catalysts were tested by ICP-MS.

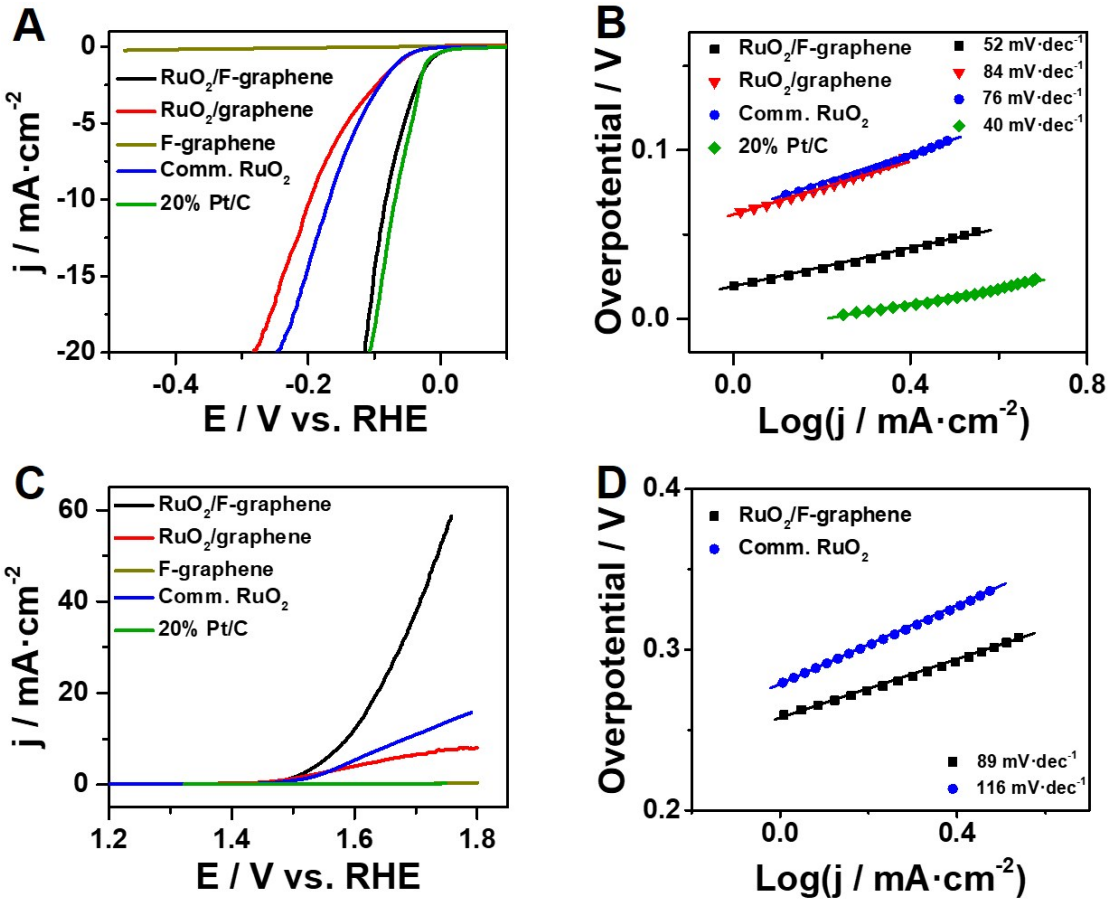

Figure S6. Electrocatalytic measurements of RuO_2/F-graphene and other catalysts in 1 M PBS solution. (A) HER performance of RuO_2/F-graphene, RuO_2/graphene, F-graphene, commercial RuO_2 and 20% Pt/C catalysts at the scan rate of 5 mV s^{-1} with iR-compensation; (B) the corresponding Tafel plots derived from (A); (C) OER performance of RuO_2/F-graphene, RuO_2/graphene, F-graphene, commercial RuO_2 and 20% Pt/C catalysts at the scan rate of 5 mV s^{-1} with iR-compensation; and (D) the corresponding Tafel plots came from (C).

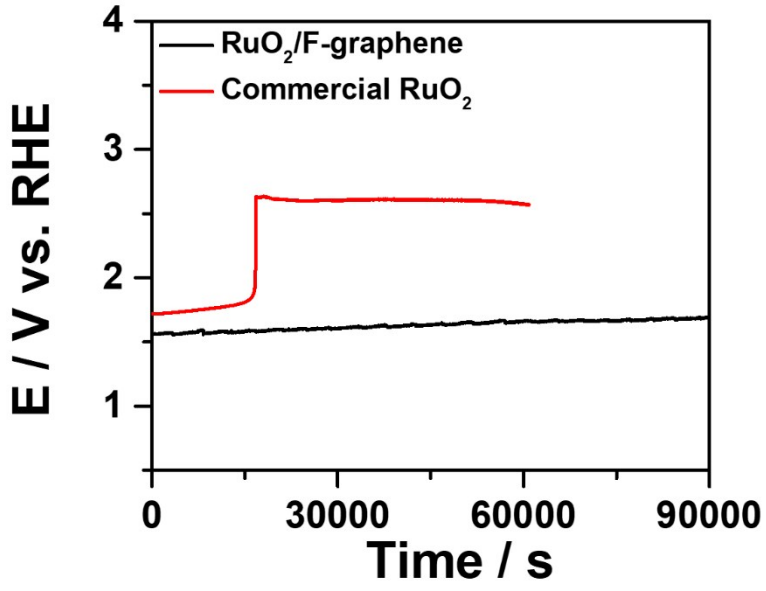

Figure S7. The long-time stability of RuO_2/F-graphene and commercial RuO_2 for overall water splitting was measured by chronopotentiometry technique and current density was maintained @ 10 $mA \cdot cm^{-2}$.

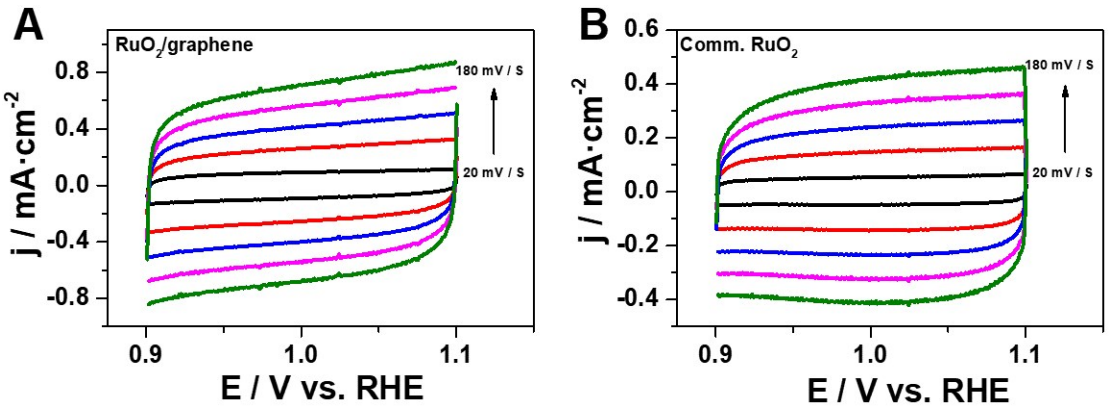

Figure S8. Electrocatalytic measurements of cyclic voltammetry (CV) under different scan rates of 20, 60, 100, 140 and 180 mV·s^{-1}. (A) CV curve of RuO_2/graphene; and (B) CV curves of commercial RuO_2.

Table S1. Comparison of different catalysts in 1 M KOH solution for HER.

Catalysts	Overpotential @ -1 mA·cm^{-2} (mV)	Overpotential @ -10 mA·cm^{-2} (mV)	Tafel slope(mV·dec^{-1})	TOF at η= 0.1 V (s^{-1})
RuO_2/F-graphene	14.2	49	31	6.60
RuO_2/graphene	18.5	119	53	0.82
Comm. RuO_2	60.5	148	81	0.02
20% Pt/C	25.8	65	40	1.40

Table S2. Comparison of different catalysts in 1 M KOH solution for OER.

Catalysts	Overpotential @ 1 mA·cm^{-2} (mV)	Overpotential @ 10 mA·cm^{-2} (mV)	Tafel slope (mV·dec^{-1})	TOF at η = 0.3 V (s^{-1})
RuO_2/F-graphene	177	239	56	2.18
RuO_2/graphene	260	360	79	0.01
Comm. RuO_2	290	380	90	0.09

Table S3. The comparison of Ru-based electrocatalysts toward HER and OER with different content of Ru.

Types	**Catalysts**	**Content of Ru (wt %)**	**Overpotential @ 10 mA·cm^{-2} (mV)**	**Tafel slope (mV·dec^{-1})**	**References**
HER	RuO_2/F-graphene	6.9	49	31	This work
	Ru-RuO_2 /CNT	64	12	30	[S3]
	RuO_2/NiO/NF	52	22	31.7	[S4]
	Ru@GnP	18.7	22	28	[S5]
	Ru/P	21.4	17	34	[S6]
	Ru NP/C	23.4	52	33	[S7]
	RuCoP	17.7	23	37	[S8]
	Ru_2Ni_2 SNs/C	13.8	40	23.7	[S9]
OER	RuO_2/F-graphene	6.9	239	56	This work
	Ru-RuO_2/CNT	64	210	64	[S3]
	Ru_2Ni_2 SNs/C	13.8	310	75	[S9]
	Ru-RuP_x-Co_xP	18.7	291	85.4	[S10]
	Ru NWs	97.9	224	46	[S11]

Table S4. Comparison of different catalysts with RuO_2/F-graphene in alkaline medium for overall water splitting.

Catalysts	Electrolyte	Current ($mA \cdot cm^{-2}$)	Potential (V)	Reference
RuO_2/F-graphene	1 M KOH	10	1.56	This work
$NiCo_2O_4$	1 M NaOH	10	1.65	[S12]
MoS_2/Ni_3S_2	1 M KOH	10	1.56	[S13]
NiS/Ni foam	1 M KOH	10	1.64	[S14]
NiCoP	1 M KOH	10	1.58	[S15]
NiCoP/rGO	1 M KOH	10	1.59	[S16]
$CoSe_2$/CF	1 M KOH	10	1.63	[S17]
RuO_2/Co_3O_4	1 M KOH	10	1.645	[S18]
MoS_2-Ni_3S_2	1 M KOH	10	1.50	[S19]
NiCoFe	1 M KOH	10	1.55	[S20]
Cu@CoFe	1 M KOH	10	1.681	[S21]

References

S1 M. W. Shao, Y. Y. Shan, N. B. Wong and S. T. Lee, Silicon nanowire sensors for bioanalytical applications: glucose and hydrogen peroxide detection. *Adv. Funct. Mater*., 2005, **15**, 1478-1482.

S2 Y. C. Pi, Q. Shao, P. T. Wang, J. Guo and X. Q. Huang, General formation of monodisperse IrM (M = Ni, Co, Fe) bimetallic nanoclusters as bifunctional electrocatalysts for acidic overall water splitting. *Adv. Funct. Mater*., 2017, **27**, 1700886.

S3 H. S. Park, J. Yang, M. K. Cho, Y. Lee, S. Cho, S. D. Yim, B. S. Kim, J. H. Jang and H. K. Song, RuO_2 nanocluster as a 4-in-1 electrocatalyst for hydrogen and oxygen electrochemistry. *Nano Energy*, 2019, **55**, 49-58.

S4 J. L. Liu, Y. Zheng, Y. Jiao, Z. Y. Wang, Z. G. Lu, A. Vasileff and S. Z. Qiao, NiO as a bifunctional promoter for ruo2 toward superior overall water splitting. *Small*, 2018, **14**, UNSP 1704073

S5 F. Li, G. F. Han, H. J. Noh, I. Ahmad, I. Y. Jeon and J. B. Baek, Mechanochemically assisted synthesis of a ru catalyst for hydrogen evolution with performance superior to pt in both acidic and alkaline media. *Adv. Mater*., 2018, **30**, 1803676.

S6 J. Yu, Y. N. Guo, S. X. She, S. S. Miao, M. Ni, W. Zhou, M. L. Liu and Z. P. Shao, Bigger is surprisingly better: agglomerates of larger RuP nanoparticles outperform benchmark pt nanocatalysts for the hydrogen evolution reaction. *Adv. Mater*., 2018, **30**, 1800047.

S7 Q. Wang, M. Ming, S. Niu, Y. Zhang, G. Y. Fan and J. S. Hu, Scalable solid-state synthesis of highly dispersed uncapped metal (Rh, Ru, Ir) nanoparticles for efficient hydrogen evolution. *Adv. Energy. Mater*., 2018, **8**, 1801698.

S8 J. Y. Xu, T. F. Liu, J. J. Li, B. Li, Y. F. Liu, B. S. Zhang, D. H. Xiong, I. Amorim, W. Li and L. F. Liu, Boosting the hydrogen evolution performance of ruthenium clusters through synergistic coupling with cobalt phosphide. *Energ. Environ. Sci*., 2018, **11**, 1819-1827..

S9 J. B. Ding, Q. Shao, Y. G. Feng and X. Q. Huang, Ruthenium-nickel sandwiched nanoplates for efficient water splitting electrocatalysis. *Nano Energy*, 2018, **47**, 1-7.

S10 L. Wang, Q. Zhou, Z. H. Pu, Q. Zhang, X. Q. Mu, H. Y. Jing, S. L. Liu, C. Y. Chen and S. C. Mu, Surface reconstruction engineering of cobalt phosphides by Ru inducement to form hollow Ru-RuPx-CoxP pre-electrocatalysts with accelerated oxygen evolution reaction. *Nano Energy*, 2018, **53**, 270-276

S11 J. Yang, Y. J. Ji, Q. Shao, N. Zhang, Y. Y. Li and X. Q. Huang, A universal strategy to metal wavy nanowires for efficient electrochemical water splitting at pH-universal conditions. *Adv. Funct. Mater*., 2018, **28**, 1803722.

S12 X. Gao, H. Zhang, Q. Li, X. Yu, Z. Hong, X. Zhang, C. Liang and Z. Lin, Hierarchical $NiCo_2O_4$ hollow microcuboids as bifunctional electrocatalysts for overall water-splitting. *Angew. Chem. Int. Ed.,* 2016, **55**, 6290–6294.

S13 J. Zhang, T. Wang, D. Pohl, B. Rellinghaus, R. H. Dong, S. H. Liu, X. D. Zhuang and X. L. Feng, Interface engineering of MoS_2/Ni_3S_2 heterostructures for highly enhanced electrochemical overall-water-splitting activity. *Angew. Chem. Int. Ed.,* 2016, **55**, 6702-6707.

S14 W. Zhu, X. Yue, W. Zhang, S. Yu, Y. Zhang and J. Wang, Nickel sulfide microsphere film on Ni foam as an efficient bifunctional electrocatalyst for overall water splitting. *Chem. Commun*., 2016, **52**, 1486-1489.

S15 H. F. Liang, A. N. Gandi, D. H. Anjum, X. B. Wang, U. Schwingen-schlogl and H. N. Alshareef, Plasma-assisted synthesis of NiCoP for efficient overall water splitting. *Nano Lett*., 2016, **16**, 7718-7725.

S16 J. Y. Li, M. Yan, X. M. Zhou, Z. Q. Huang, Z. M. Xia, C. R. Chang, Y. Y. Ma and Y. Q. Qu, Mechanistic insights on ternary Ni_2-xCoxP for hydrogen evolution and their hybrids with graphene as highly efficient and robust catalysts for overall water splitting. *Adv. Funct. Mater*., 2016, **26**, 6785-6796.

S17 C. Sun, Q. Dong, J. Yang, Z. Dai, J. Lin, P. Chen, W. Huang and X. Dong, Metal-organic framework derived $CoSe_2$ nanoparticles anchored on carbon fibers as bifunctional electrocatalysts for efficient overall water splitting. *Nano Research,* 2016, **9**, 2234-2243.

S18 H. Liu, G. Xia, R. Zhang, P. Jiang, J. Chen and Q. Chen, MOF-Derived RuO_2/Co_3O_4 heterojunctions as highly efficient bifunctional electrocatalysts for HER and OER in alkaline solutions. *RSC Adv*, 2017, **7**, 3686-3694.

S19 Y. Yang, K. Zhang, H. Lin, X. Li, H. C. Chan, L. Yang and Q. Gao, MoS_2-Ni_3S_2 heteronanorods as efficient and stable bifunctional electrocatalysts for overall water splitting. *ACS Catal*., 2017, **7**, 2357-2366.

S20 A. L. Wang, H. Xu and G. R. Li, NiCoFe Layered Triple Hydroxides with Porous Structures as High-Performance Electrocatalysts for Overall Water Splitting. *ACS Energy Lett*., 2016, **1**, 445-453.

S21 L. Yu, H. Zhou, J. Sun, F. Qin, D. Luo, L. Xie, F. Yu, J. Bao, Y. Li, Y. Yu, S. Chen and Z. F. Ren, Hierarchical Cu@CoFe layered double hydroxide core-shell nanoarchitectures as bifunctional electrocatalysts for efficient overall water splitting. *Nano Energy,* 2017, **41**, 327-336.